UNIVERSITAT DE BARCELONA

Field-effects on single molecular circuitry

Electronic transport from synthetic to biological models

Albert Cortijos i Aragonès

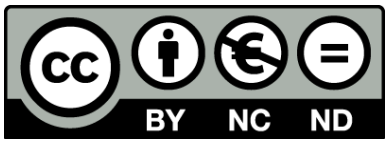

Part II

ELECTRIC FIELDS IN SINGLE-MOLECULE

Chapter 5

Effects of the Electric Fields: *Tunning the Reaction*

Catalysis improves the chemical processes making them faster, cheaper and more efficient, so we can consider it like an essential pillar of our society because affect to any aspect of our lives, from food production to cosmetics, technology, medicines or any employed material; in fact, has been estimated that 30-40% of the planetary *gross world product* depends on catalytic processes.[539] Besides, the catalysis in biological processes called enzymatic, represents the most efficient catalytic processes as was explained in the introduction (Page 51), and they affect to the majority of the reactions in biology, thus study them not only will help to the medical field, but also will affect on the *fine chemicals* production where they are very-well established and their use is growing day by day,[540–542] nevertheless any improvement on enzymatic processes will seriously impact on one of the economic giants of the present times, the Bio-Manufacturing industry, due its strongly dependence on such processes.

As a direct consequence, understand the EEF effects on molecules and how to turn them to a catalytic *force fields* has become one of the major scientific and technical challenges of our era.[539,543] To achieve it, the "electrostatic catalysis" tries to manipulate the chemical reactions through the effects of an electrostatic field consequence of a directional electric field. As was detailed in the introduction (Page 50), such phenomenon can be explained using Shaik's model where the EEF in a chemical reaction orients the charge-separated resonance contributors of the Transition State (TS), electrostatically stabilizing them therefore catalyzing the reaction."Electrostatic catalysis" also can be used to explain the phenomenology and many fundamental effects behind the enzymatic processes, because the mechanistics attributed to such biological processes has been straightly associated[245,246,256,257,544] to the presence of LEFs, originated in the enzyme's active sites cages thanks to the cooperatively disposition of one or more than one charged residues, aimed to orient the substrate molecules to force an efficiently binding.[241,242]

Regarding the explained reasons along with the Electrostatic Catalysis' need to get a robust platform (Page 53) used to study the associated phenomena, this Chapter's research has as a *first objective*, the development of this required **new molecular platform** which allow the application of EEFs in a controlled way defining their strength and orientation between reactant molecules, aimed to create a molecular junctions with the reaction product molecules. Then, as a *second objective*, and maybe a bit far from the original propose (Page 36) using the new developed platform strictly on molecular circuitry purposes, such platform will be employed to study the **EEF effect in a chemical reaction** based on molecular junctions between reactant molecules, expanding the fundamentals and potential uses of the "electrostatic catalysis" which can also help to elucidate the LEF behind the enzymatic processes and their improvement via employing the EEF.[245,246,257,260–263] Despite the most ambitious target is to deepen the mentioned enzymatic processes, due the complexity and the huge number of interfering factors that should be handled using biological structures, they do not represent a valid molecular ideal model for a straightforward fundamental research at the first stages, for this reason the presented work is focused on a bimolecular non-enzymatic reaction.

"Electrostatic catalysis" experimental precedents[245,246,256–258] in non-enzymatic processes did not show efficient results despite they particularly overcame some associated problems like the field's directionality quenching (see the explanation on previous Page 51); these first bulky scale experimental attempts were strongly inspired on the commented biological models where the enzymes uses active sites to create a well defined oriented field, forcing the substrate to bind in a specific way. Such experiments consisted in the attachment of charged functional groups[241,242,545,546] in a specific disposition on the catalyst surface allowing to create a local electrostatic field.[251,545,546] Since the electrostatic fields are highly directional, the reactant molecules were orientated in a specific manner to favor the reaction. Furthermore, since the drawback related to the highly directional local fields quenched in polar media[547] is sort it out by employing solvents of low polarity, as a consequence is decreased the solubility of the charged residues thus reducing the reaction rate and the applicability of the method.[547,548]

As illustrated above, "electrostatic catalysis" studies performed at the macroscale present dependence on the electric fields but were achieved with an evident low efficiency in comparison with the analogous biologic enzymatic systems (see Figure 5.1) due the impossibility to create an optimal structural environment like the enzymatic cages, thus affecting to control the LEFs, a practical difficulty which impede a real extended implementation.

Recently, different strategies at the bulk scale have been develop, such as the design of task-specific ionic liquids to make the catalytic processes more efficient[549] or the use of semiconducting electrodes,[550] but the control of EEF to the *nanoscale* level represent the most promising way to proceed through. Still following Shaik's model, the EEF can be used kinetically and thermodynamically to tune the reactivity behaving as a "conventional" *catalyst* chemical specie.[551] Few precedents

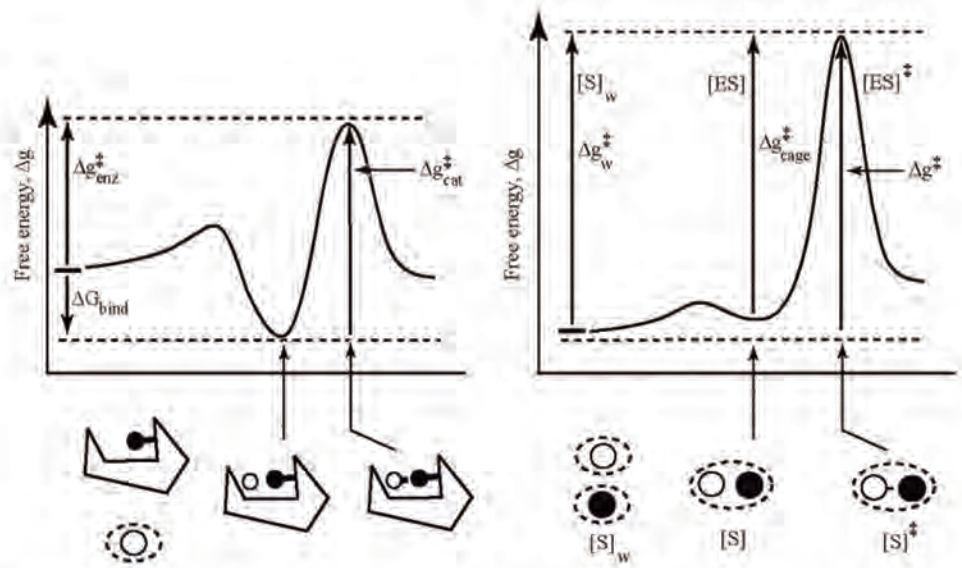

Figure 5.1: Schematic description of the free energy profile for an enzymatic reaction and that for the corresponding non-enzymatic "electrostatically catalyzed" reaction. Adapted from Warshel et al.[256]

used this idea at the monolayer level employing the EEF to catalyze isomerization reactions through the control of transition polar states[260,552] or the molecular rearrangement through molecular intermediates,[230] although the cited works represent the state-of-the-art research of the field, the applicability still being very limited since the reaction is conducted on established molecules rather than employing the usual chemical reaction between two reactant molecules "colliding" and generating a new one (bimolecular reaction), as is the case for the majority uses for applied chemistry. For this reason the aim of this Chapter is the application of the EEF on the well-know Diels-Alder bimolecular reaction.[240,553] Diels-Alder is one of the

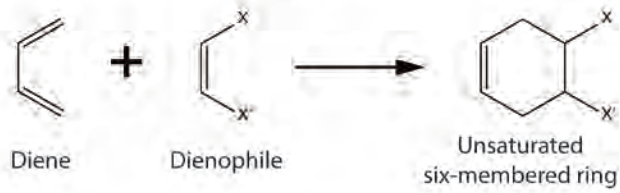

Figure 5.2: Diels-Alder reaction schematic representation between a diene and a dienophile and an unsaturated six-membered ring as the product molecule.

most studied chemical reactions, and consists in a carbon-carbon bond-forming reaction between a *diene* and a *dienophile* (Figure 5.2). This reaction was developed in the 1928 in the *Humboldt* University of Berlin, however, still widely used nowadays dominating the industrial synthesis,[553–557] e.g is implied on many steps for the production of rubber and plastic materials as well as in the elaboration of fragrance bases and concentrates, perfumes and colognes, is used in soaps, hygiene products,

cosmetic preparations, air fresheners, textile detergents, cleaning products and also for the flavor and fragrance industry;[555] also is involved on the production more than 2400 active pharmaceutical ingredients[556,558] among those are a produced in *Industrial-Scale Synthesis* (Kg production scale) like vitamins and prostaglandins.[557]

Focusing in its reactivity, since the Diels-Alder reaction is not a redox reaction and do not involve electroactive species but is affected by the EEF.[251,543] Such influence has been extensively studied by quantum chemistry, specially focusing on its dependence to the applied field orientation which can decrease or increase substantially the barrier heights (see Figure 5.3) and therefore accelerating or decreasing the reaction efficiency[243,251,543] as Shaik and others propose extensively in their theoretical studies.[240,243,245,253] Given these broad preceding theoretical studies as background and the structural simplicity of the reactant molecules, in this Chapter the Diels-Alder reaction represents the most suitable model reaction to study the EEF effects on reactivity at single-molecule scale employing the STM microscope as characterization tool via molecular conduction experiments at RT, as it follows.

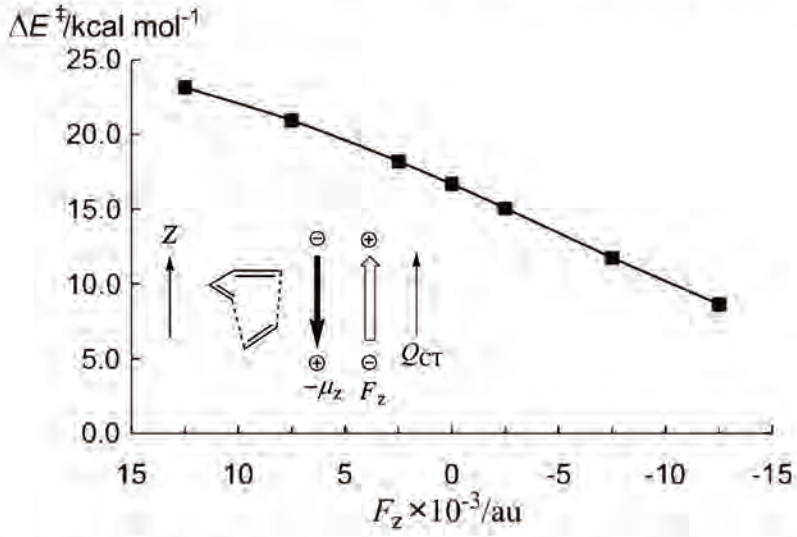

Figure 5.3: Diels-Alder reaction barriers vs. the field strength in the Z-direction (F_z). Inset: F_z vector, the interaction mode of F_z with the dipole moment μ_Z (black arrow), the positive F_z direction (empty arrow) and Q_{CT} vector shows the amount of charge. Adapted from Meir et al.[240]

5.1 The experimental research

Thanks the STM *two-electrodes* design and its robust and stable single-molecule STM-BJ technique (see *Section "STM Break-Junction Technique"*, on Page 26), in this research a tunable EEF stimulus at RT could be applied between two reactant molecules attaching them separately to both tip and substrate electrodes.[482] Such employed molecules were the non-polar *dienophile*, a *(±)-norbornylogous bridge (NB),tricyclo [4.2.1.0^{2,5}] non-7-ene-3,4-dimethanethiol* molecule attached to the Au(111) electrode substrate's surface and the *diene*, a *2-methyl-3-furanthiol* molecule, attached to the Au tip. Both reactant molecules were synthesized on propose[47,559–562] and presented ostensibly negligible polarity and were measured under mesitylene, as the apolar organic medium. A detailed description of the sample, substrate and tip preparation can be found from Page 328 (*Appendix C.2*).

EEF represented the main parameter used to control the proposed experiments and employing the STM was easy tunned through the applied bias voltage between tip and substrate electrodes. Its magnitude defined the strength of the EEF, and its polarity defined the orientation of the EEF, i.e *from tip-to-substrate* EEF due the application of negative bias voltages and *from substrate-to-tip* EEF due positive bias voltages. The formation of product molecules was detected via current measurements, thanks to the determination of the current signature of this product molecules bridged between the two electrodes was possible the (electrical) monitoring of current events corresponding to *in-situ* reaction events. Quantifying the frequency of the detected current events in a given time interval, allowed to obtain a direct analogy to the reaction rate, thereby any effect caused as a consequence of the EEF strength and orientation could be captured and studied.

In this experiments the two STM-BJ approaches were used, the static *blinking* and the dynamic *tapping* (see *Appendix C.1*, Page 325 for a detailed explanation). Their inherent differences defined their applicability and usefulness. In the *blinking* approach the tip and substrate electrodes kept the distance according to the the molecule product length (ca. 1 nm) between them in a very stable motionless way, this allows the spontaneous formation of the Diels-Alder product molecules meanwhile the current is continuously captured,[94,95] reason why is the most accurate way to obtain the reaction rates. However, since the typical amount of captured data with the *blinking* approach is low in comparison with the *tapping* dynamic approach, the latter was used as supporting technique because can statistically reinforce any trend observed via the *blinking* approach, as was explained in previous Chapters. Despite this, the *tapping* approach in some circumstances should used as a merely support because it sacrifices stability to acquire statistics through the mechanically forced junction formation and breakdown. In this case it can avoid the desired spontaneous reactions and lacks on any kind of junction information. The two different approaches are mutually complementary to achieve the same aim, the detection of current signals and associate them to the molecular formation events of the Diels-Alder reaction under variable EEF strength and orientation conditions.

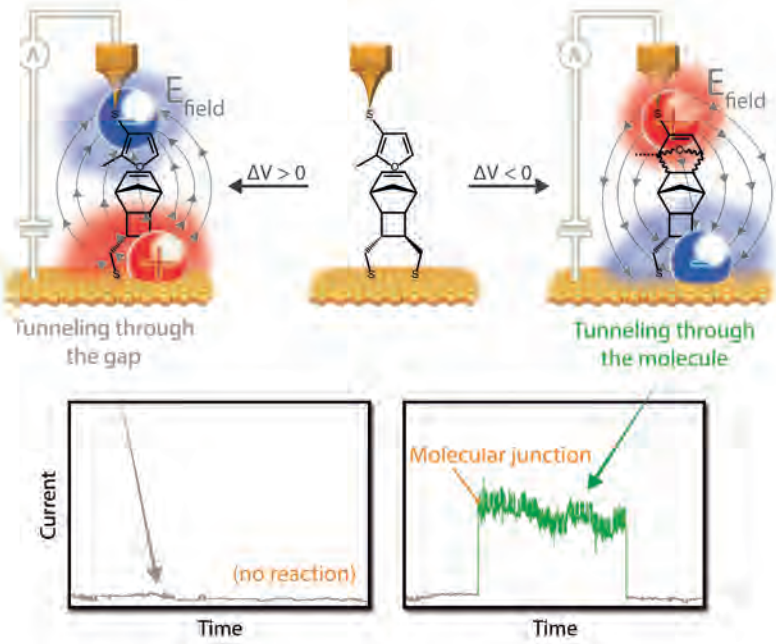

Figure 5.4: Idealized representation where the Diels-Alder reaction reactants and product molecules are attached the STM tip and substrate under two possible scenarios according to the electric filed orientation. At the bottom are shown the two currant responses associated to the current through the gap, due no reaction events (left) and through the molecule product due the Diels-Alder reaction (right).

According to the previous theoretical studies, the expected phenomenology for the presented experiments can be summarized as the reaction rate increment depending on the bias voltage polarity (EEF orientation) and proportional to its magnitude (EEF strength). Thus, tunning the magnitude of the bias voltage between the electrodes along with the current sense inversion (polarity), the frequency of the detected current events should be affected, allowing to study the variations of the reaction rates through it. Such idealized scenarios are represented on Figure 5.4. In the presented work in the following pages all the experimental research was supported thanks to a strong support of quantum chemistry computational calculations, with the fundamental objective to determine mainly the consequences of the EEF strength and orientation to the Diels-Alder reaction and elucidate of the affected parameters like the reaction rate. High-level G3(MP2,+,CC) was used to study the molecular systems and M06-L/cc-pVTZ to study the reaction barriers of the formation products.

5.2 Objectives and Summary of the experimental work

- Using the static *blinking* approach, were applied different magnitude and polarity biases from +0.050 V to +0.750 V and from -0.050 V to -0.750 V, controlling in this way the effects of the orientation and electric field strength. The total captured time for each bias voltage value was of 8 hours.

- The dynamic STM-BJ *tapping* approach was used to perform thousands of junctions under the same bias voltage conditions employed with the previous *blinking* approach, to confirm the observed effects obtained by the latter thanks of its statistical robustness due the accumulated information from the performed junctions.

- Many control experiments were performed to find a unequivocal assignation of the current signature to the Diels-Alder product molecules, performing controls where the reaction was not allowed. In order to do it were employed both approaches under the previous experimental conditions but using saturated furan molecules replacing the aromatic furan, as well as employing saturated norbornylogous bridge molecules replacing the NB dienophile. Besides, with the same objective and using again both approaches under the same conditions, were performed the experiments within the absence of either reactant from the tip or from the surface.

- To ascertain unequivocally the establishment of the molecular single-molecule connection of the product molecule between the two Au electrodes, mechanical pullings over a *blinking* events were exerted. This procedure presented in previous Chapters (and explained on *Appendix C.1*, Page 325) is based on a mechanical retraction of the Au tip electrode, in this case was withdrawed more than 1 nm (ca. Diels-Alder product molecule length). As a reference of a junction-free scenario also was applied the same procedure under a tunneling current through the gap and immediately after the application the current decayed to zero value.

In the following pages is shown summarized the research as a published paper and its Supplementary Information reduced to the experimental Section as a consequence of the extension of the molecular synthesis, characterization and computational data (see on-line complete version at `http://www.nature.com/nature/journal/v531/n7592/full/nature16989.html` *):*

"A.C. Aragonès, N.L. Haworth, N. Darwish, S. Ciampi, N.J. Bloomfield, G.G. Wallace, I. Diez-Perez, and M.L. Coote. Electrostatic catalysis of a Diels-Alder reaction. *Nature*, 531(7592):88–91, 2016".

LETTER

doi:10.1038/nature16989

Electrostatic catalysis of a Diels–Alder reaction

Albert C. Aragonès[1,2,3], Naomi L. Haworth[4], Nadim Darwish[1,2], Simone Ciampi[5], Nathaniel J. Bloomfield[4], Gordon G. Wallace[5], Ismael Díez-Pérez[1,2,3] & Michelle L. Coote[4]

It is often thought that the ability to control reaction rates with an applied electrical potential gradient is unique to redox systems. However, recent theoretical studies suggest that oriented electric fields could affect the outcomes of a range of chemical reactions, regardless of whether a redox system is involved[1–4]. This possibility arises because many formally covalent species can be stabilized via minor charge-separated resonance contributors. When an applied electric field is aligned in such a way as to electrostatically stabilize one of these minor forms, the degree of resonance increases, resulting in the overall stabilization of the molecule or transition state. This means that it should be possible to manipulate the kinetics and thermodynamics of non-redox processes using an external electric field, as long as the orientation of the approaching reactants with respect to the field stimulus can be controlled. Here, we provide experimental evidence that the formation of carbon–carbon bonds is accelerated by an electric field. We have designed a surface model system to probe the Diels–Alder reaction, and coupled it with a scanning tunnelling microscopy break-junction approach[5–7]. This technique, performed at the single-molecule level, is perfectly suited to deliver an electric-field stimulus across approaching reactants. We find a fivefold increase in the frequency of formation of single-molecule junctions, resulting from the reaction that occurs when the electric field is present and aligned so as to favour electron flow from the dienophile to the diene. Our results are qualitatively consistent with those predicted by quantum-chemical calculations in a theoretical model of this system, and herald a new approach to chemical catalysis.

All chemical reactions can be viewed as the movement of electrons and/or nuclei; as such, one might expect that their kinetics and thermodynamics could be influenced by external electric fields. Even for non-redox reactions, theoretical studies predict that electrostatic effects should in principle influence the stabilities of chemical species by stabilizing or destabilizing charge-separated resonance contributors[1–4]. For example, Shaik and co-workers have argued that a covalent bond of the form X–Y can be thought of as comprising several possible resonance contributors, $[XY \leftrightarrow X^{+}Y^{-} \leftrightarrow X^{-}Y^{+}]$[8,9]. In the absence of an electric field, the extent to which either of the charge-separated structures will contribute to the resonance stabilization of the bond will depend on the relative electronegativities of X and Y. Indeed, Shaik and colleagues were able to use this concept to explain energy trends in the group 14 MH_3–Cl bonds[10], among other examples. In this context, the presence of an appropriately oriented external electric field has the potential to further stabilize or destabilize these charge-transfer contributors, and thereby influence bond energy. Moreover, the participation of minor charge-separated resonance structures is not limited to covalent-bond energies; it has been invoked to explain trends in kinetics and thermodynamics for a wide range of chemical reactions, including radical addition[11] and transfer[12]. Thus, in principle, the scope of electrostatic catalysis—manipulating chemical reactions with electric fields—should be broad.

Electrostatic catalysis is the least developed form of catalysis in synthetic chemistry (even though it is widely harnessed by enzymes[13–16]). This is because electrostatic effects are strongly directional and are effectively quenched in polar media. Enzymes overcome these problems by using a low-polarity active site, in which the substrate binds in a precisely oriented manner; one or more charged residues within this site can then create an oriented local electric field that can catalyse the reaction. In synthetic chemistry, one can mimic this process to some extent by using charged functional groups on the substrate or catalyst; however, balancing the need for low solvent polarity with the limited solubility of charged residues in non-polar solvents leads to compromises that weaken the catalytic effect. For example, aminoxyl radicals ($R_1R_2NO^{\bullet}$) are stabilized via resonance with $R_1R_2N^{+}{}^{\bullet}O^{-}$. Thus, when a (remote) negatively charged functional group is placed on the left-hand side of the N–O$^{\bullet}$ bond, the electrostatic stabilization of this minor contributor leads to further stabilization of the species[2,3]. This stabilization, which has been verified experimentally, promotes dissociation of the R_1R_2NO–H and R_1R_2NO–R bonds by as much as 20 kJ mol^{-1} in the gas phase[2]; however, the effect, while still of practical significance as a 'pH switch' of radical stability, is effectively halved in energetic terms in low-polarity solvents such as dichloromethane[17], and essentially quenched in polar solvents[18].

If one could use external electric fields instead of charged chemical species as the 'catalyst', one could manipulate a much broader range of reactions, conveniently altering both reactivity and selectivity in a tunable manner that can be predicted by theory. However, to probe this concept experimentally, one must develop a method of controlling the orientation of the external electric field (EEF) with respect to the reaction centre. Previously, EEFs have been used to guide the selectivity of isomerization reactions in which polar intermediates or transition states are involved[19,20]; but controlling the orientation of the EEF as two molecules collide in bimolecular reactions adds another dimension to the problem. Here we show that this can be achieved by combining surface chemistry procedures with state-of-the-art single-molecule techniques that are based on scanning tunnelling microscopy (STM). STM-based single-molecule electrical measurements can reveal information on chemical coupling averaged over thousands of collisions. This gives us the ability to control the dynamics of the approaching reactants and deliver the field stimulus upon collision. Using this approach, we show that a simple, textbook bimolecular carbon–carbon bond-forming reaction, the Diels–Alder reaction—involving reagents of ostensibly negligible polarity—can be accelerated by an oriented EEF.

Diels–Alder reactions—which involve a conjugated diene and a substituted alkene (the 'dienophile')—constitute a major family of chemical processes that are used in the preparation of fine chemicals[21]. Our choice of these reactions was inspired by theoretical predictions by Shaik and colleagues[1], who suggested that the barrier heights for certain Diels–Alder reactions can be lowered substantially when an electric field is oriented appropriately. Here we use a

[1]Departament de Química-Física, Universitat de Barcelona, Diagonal 645, Barcelona 08028, Catalonia, Spain. [2]Institut de Bioenginyeria de Catalunya (IBEC), Baldiri Reixac 15-21, Barcelona 08028, Catalonia, Spain. [3]Centro Investigación Biomédica en Red (CIBER-BBN), Campus Río Ebro-Edificio I+D, Poeta Mariano Esquillor s/n, Zaragoza 50018, Spain. [4]ARC Centre of Excellence for Electromaterials Science, Research School of Chemistry, Australian National University, Canberra, Australian Capital Territory 2601, Australia. [5]ARC Centre of Excellence for Electromaterials Science, Intelligent Polymer Research Institute, University of Wollongong, Wollongong, New South Wales 2500, Australia.

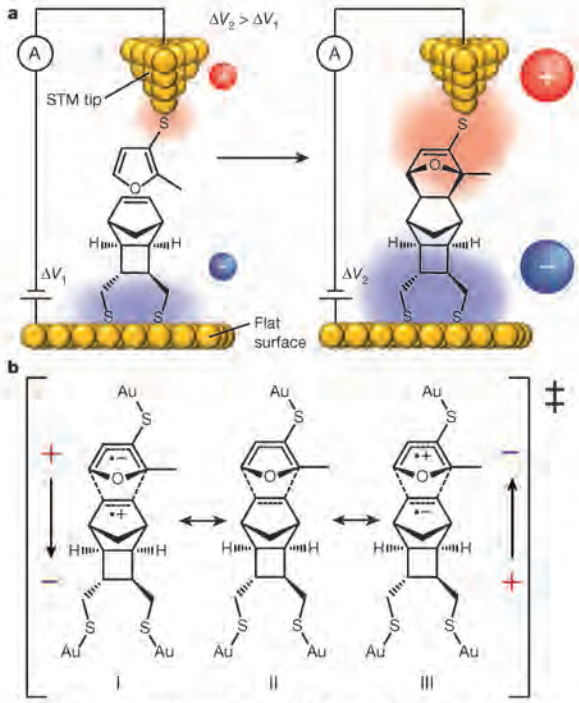

Figure 1 | Electrostatic catalysis of a Diels–Alder reaction. a, We studied the effects of an external electric field on the reaction rate by using single-molecule STM-BJ conductance measurements, which provide the oriented electric-field stimulus and also count reaction events. The diene (a furan) is attached to the STM tip via a thiol group ('S'); the dienophile (a norbornylogous bridge) is attached in a known orientation[26] to a flat gold surface via two thiols. Four structurally distinct products may be formed, each having two diastereoisomers; the kinetically favoured product is shown here. ΔV is the voltage difference between the tip and surface electrodes. **b**, Possible resonance structures of the transition state. When an electric field is present, minor contributors I or III may be stabilized enough to undergo resonance with II, lowering the reaction barrier. The vertical arrows show the field direction most likely to stabilize I or III, with I expected to experience greater stabilization at a given field magnitude.

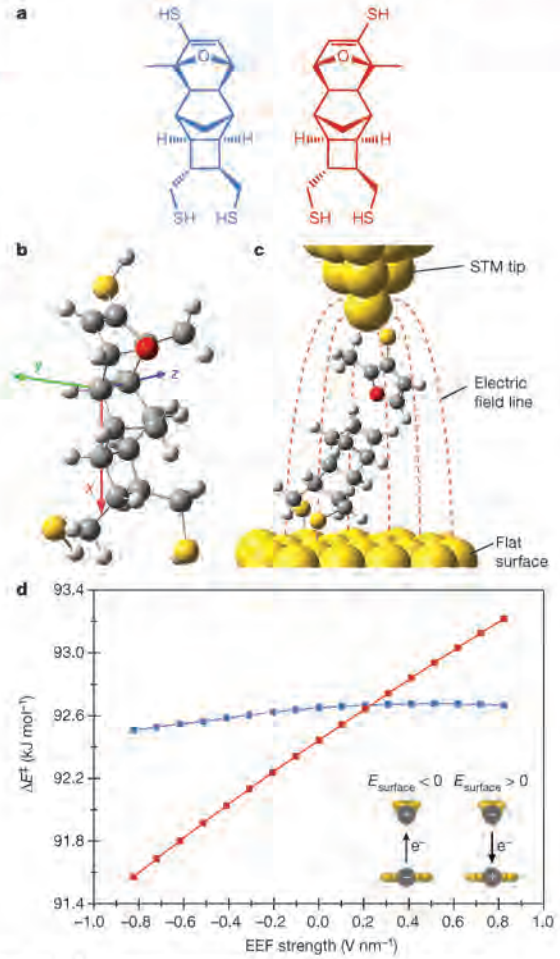

Figure 2 | Computational modelling of the Diels–Alder reaction. a, The two diastereoisomers of the *exo–syn* product of this reaction. These were the kinetically favoured products; the six other possible products had much higher reaction barriers over the experimental range of field strengths. In the blue diastereomer, the substituents of the furan are located on the left of the molecule; in the red diastereomer, these substituents are located on the right. **b**, The coordinate axes used to orient the field with respect to the molecule. The *z* axis lies along the double bond of the dienophile, while the *x* axis is directed along the **NB** backbone. **c**, The scenario being modelled, showing the **NB** bridge sitting in the experimentally determined orientation with respect to the surface of the STM plate and to the electric field lines, which are passing through the reaction centre at an oblique angle to the **NB** double bond. **d**, The predicted effects of the strength and direction of the external electric field (EEF) on the reaction-barrier height ($\Delta E^{\ddagger}$) for formation of the two *exo–syn* diastereoisomers in **a** (see Supplementary Information). The formation of the blue structure is quite insensitive to the EEF over the experimental range of field strengths, while the formation of the red structure shows strong field sensitivity. The diagrams in the bottom right corner show the possible directions of the electric field (where $E_{surface}$ denotes the voltage applied between the surface and the tip).

surface-tethered furan derivative as the diene, and a norbornylogous bridge with a terminal double bond as a non-polar dienophile ((±)-**NB**, tricyclo[4.2.1.0^{2,5}]non-7-ene-3,4-dimethanethiol; only the (1(*R*),2(*R*),3(*R*),4(*R*),5(*S*),6(*S*))-enantiomeric form is shown in Fig. 1a). Norbornylogous bridges are conformationally rigid molecules, and have been extensively used as electrical conduits for probing how geometrical and structural factors influence chemical and electrochemical phenomena[22–24]. The **NB** in Fig. 1a is a short, rigid, non-polar dienophile with two CH_2SH groups (feet) in *trans*-stereochemistry; the presence of these feet allows unambiguous orientation of the distal double bond (dienophile) when assembled on flat gold surfaces[23,25]. The rigidity of **NB** helps us to position and align the dienophile with respect to the EEF when the diene part of the system is brought nearby. The molecular length of the dienophile is kept to a minimum (five sigma bonds) in order to maintain the Diels–Alder product within the conductance limit of our system.

To ascertain whether this Diels–Alder reaction is sensitive to the presence of an oriented EEF, we used quantum chemistry to study the field effect on the reaction barrier. This reaction has four structurally distinct Diels–Alder products; results for the reaction with the lowest barrier (*exo–syn*) are shown in Fig. 2 (see Supplementary Information for full results). There are two diastereoisomers for each of the four products, with the substituents of the furan being located either on the left of the molecule (see the blue diastereomer in Fig. 2a) or on the right (the red diastereomer).

The positioning of these substituents leads to different interactions with the CH_2SH groups at the opposite end of the **NB**, resulting in slightly different energies when no EEF is present and very different responses to the applied field. Experimentally, the **NB** is known to sit at

RESEARCH LETTER

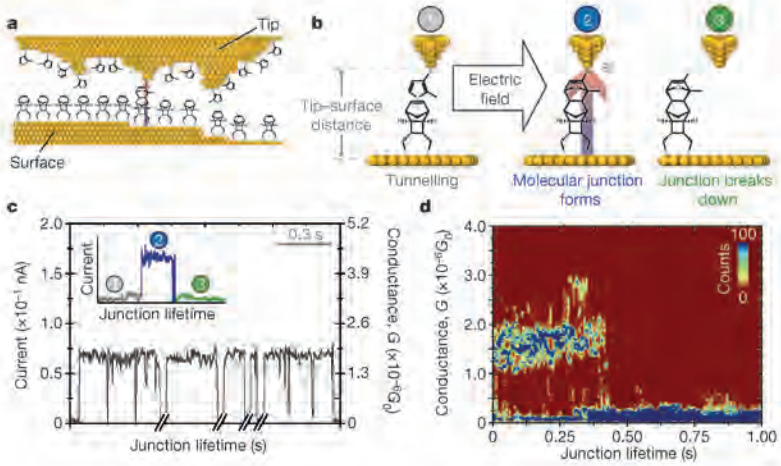

Figure 3 | Blinking experiments. a, Diagram of the STM tip and surface during a blinking experiment. The STM tip was modified by furan molecules and the surface with **NB** molecules, using self-assembled-monolayer procedures (see Supplementary Information). **b**, The stages encountered during a blinking event. **c**, A real-time data capture of blinking events. The time breaks in the *x* axis are about 2 min. The inset shows the STM current response before (1), during (2) and after (3) the formation of a single blink (junction). **d**, Two-dimensional maps overlaying hundreds of blinks. Counts have been normalized to a colour scale, with 100 counts representing the maximum, and 0 representing the minimum. The surface bias was −0.5 V in **c**, **d**. $G_0 = 2e^2/h = 77.5\,\mu S$, with h the Planck constant and e the elementary charge.

an angle to the gold surface[26], tilted by 30° along the *y* axis and 25° along the *z* axis (Fig. 2c). For the *exo–syn* product, the 30° *y*-axis tilt means that the field lines are oriented roughly along the average vector of the forming bonds. However, the *z*-axis tilt means that the furan SH group sits above the forming bonds for the blue diastereoisomer (Fig. 2c), but to the side of the molecule for the red diastereoisomer. As a result, the blue structure is predicted to be quite insensitive to the EEF over the experimental range of field strengths, while the red structure should show strong field sensitivity (see Supplementary Information, section 3). Specifically, it is predicted that, for negative bias, the barrier to formation of the red isomer will decrease with increasing field strength; for positive bias, it is predicted to increase (Fig. 2d). This trend occurs because the negatively biased EEF can stabilize resonance contributor I (Fig. 1b); a positively biased field will destabilize it. In principle, a positively biased field should also lower the barrier height by stabilizing resonance contributor III. However, configuration III has much less inherent stability than contributor I, as the electronegative oxygen prefers to bear a negative rather than a positive charge. As a result, this configuration contributes only at strong positive fields, outside of the experimental range (see Supplementary Figs 3–8). Within the experimental range, our calculations predict that the frequency of adduct formation should increase systematically as the strength of the negatively biased field increases, up to a factor of 1.5 at −0.75 V, while remaining relatively independent of EEF strength for positively biased fields.

To test these predictions experimentally, we attached the **NB** to the surface of a flat gold electrode, and the furan to the STM gold tip. We then undertook a series of STM break-junction approach (BJ) experiments known as 'blinking'[7,27]. The blinking technique detects the formation of molecular bridges between an STM tip and a substrate electrode—while they are fixed at a specific electrode–electrode distance—by imposing an initial set-point tunnelling current (Fig. 3 and Supplementary Information, section 2). After the set-point current is reached, the feedback loop is turned off and the current is monitored. Current jumps (blinks) appear when a molecular bridge spans the gap between the electrodes (Fig. 3c). We detected blinks in conductance of magnitude $(1.5–2) \times 10^{-6} G_0$ when the tip and substrate were separated by a distance that allows the Diels–Alder reaction to occur (about 1 nm). These junctions formed only when both reactants were present. When either reactant was removed from its respective electrode, or when their saturated analogues were used (2-methyl-3-tetrahydrofuranthiol on the tip, or a hydrogenated version of **NB** on the surface—a system that is structurally identical but which lacks the diene–dienophile character), there was no evidence of molecular-bridge formation (Supplementary Information, section 2). Hence, the junctions are formed through the Diels–Alder reaction. At positive voltage biases (surface positive), the frequency of molecular-bridge formation is constant (five blinks per hour) over a wide range of applied biases. In contrast, at negative biases the frequency is clearly affected by the strength of the field, and increases from five blinks per hour at a bias of −0.05 V, to 25 blinks per hour at a bias of −0.75 V (Fig. 4). These trends are in complete qualitative agreement with the theoretical predictions in Fig. 2d. Quantitatively, there are differences, which may relate to the difference in the realms being studied experimentally and computationally (single-molecule reaction rates versus bulk reaction rates), and/or the use of pre-complexes in calculating field effects on barrier heights (see Supplementary Information).

As further validation that the experiment is detecting the formation of carbon–carbon bonds, we note that the average lifetime of the blinks was 0.4 s (Fig. 3d), with poor dependence on the electric-field magnitude for positive biases up to 0.75 V (Supplementary Information, section 2). This lifetime is around the same as that observed for standard single-molecule wires that are thiolated at both ends[6,24]. A bias value higher than +0.75 V or lower than −0.75 V led to a drop in the lifetime of the junctions, owing to the instability of the gold–sulfur contacts. Hence, we kept the upper limit of the bias within the range +0.75 V to −0.75 V, to allow us to compare different biases while maintaining similar junction stabilities. We also confirmed the formation of mechanically stable carbon–carbon bonds by collecting pulling curves during the blinking events (Supplementary Figs 2–6), or by performing pushing/pulling cycles (Supplementary Figs 2–7). Pulling curves collected over the blinks showed a plateau with an average pulling length of 0.2 nm, which corresponds to the stretching of the single-molecule bridge. When the pulling was exerted over the tunnelling background or on random noise (Supplementary Figs 2–6), a clean exponential decay was observed, testifying that the above blinks are attributable to a stable molecular junction, rather than resulting from the migration of gold atoms or from fluctuations in molecular conformations[28,29].

We further confirmed that robust molecular junctions were formed using an STM-BJ approach[5,30] referred to as tapping. Here, the furan-modified tip was repeatedly driven into and out of contact with the **NB**-modified substrate (Supplementary Figs 2–7): when the reactants were mechanically brought together, molecular junctions formed; when the tip was pulled away, the junctions broke. During the pulling portion of the cycles, we detected plateaus in the current-versus-distance curves of the same conductance magnitude as that observed in the blinking experiments ($(1.5–2) \times 10^{-6} G_0$; Supplementary Information, section 2 and Supplementary Figs 2–7), further supporting the idea that stable molecular wires form when the two reactants are brought together under an electric field. Moreover, changes to the magnitude and direction of the field applied across the reactants affected the rate of the Diels–Alder reaction in a similar manner to that found via

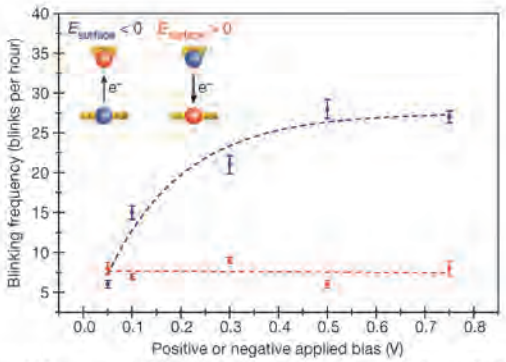

Figure 4 | Frequency of blinks (junctions) as a function of the applied bias. Positive and negative biases are plotted in red and blue, respectively. To keep the distance between the surface and the tip constant across the bias range, we used the same set-point current and changed the bias while the STM feedback was turned off. We performed blinking experiments over periods of one hour. At the end of each one-hour period, we changed the furan-modified STM tip and its lateral position with respect to the surface to compensate for the loss of reactants. We repeated this procedure eight times, giving each bias point (magnitude and direction) a total experimental time of eight hours. We changed the chronology of the selected biases randomly for each repeat. Error bars represent the standard deviation from the eight (one-hour) intervals. The dashed lines are included for visual guidance.

blinking. Tapping data show that product formation increases by 4.4-fold, from 4.2% (252 product molecules out of 6,000 attempts) to 18.6% (1,116 product molecules out of 6,000 attempts) when the surface bias is changed from −0.05 V to −0.75 V (Supplementary Figs 2–7).

We have presented the first (to our knowledge) experimental evidence of a non-redox, bond-forming process being accelerated by an oriented EEF. Our experimental results are qualitatively consistent with theoretical calculations, and result from the ability of the electric field to electrostatically stabilize a minor charge-separated resonance contributor of the transition state. This ability to manipulate chemical reactions with electric fields offers proof-of-principle for a change in our approach to heterogeneous catalysis.

Received 16 May 2015; accepted 7 January 2016.

1. Meir, R., Chen, H., Lai, W. & Shaik, S. Oriented electric fields accelerate Diels–Alder reactions and control the endo/exo selectivity. *ChemPhysChem* **11,** 301–310 (2010).
2. Gryn'ova, G., Marshall, D. L., Blanksby, S. J. & Coote, M. L. Switching radical stability by pH-induced orbital conversion. *Nature Chem.* **5,** 474–481 (2013).
3. Gryn'ova, G. & Coote, M. L. Origin and scope of long-range stabilizing interactions and associated SOMO–HOMO conversion in distonic radical anions. *J. Am. Chem. Soc.* **135,** 15392–15403 (2013).
4. Shaik, S., de Visser, S. P. & Kumar, D. External electric field will control the selectivity of enzymatic-like bond activations. *J. Am. Chem. Soc.* **126,** 11746–11749 (2004).
5. Xu, B. & Tao, N. J. Measurement of single-molecule resistance by repeated formation of molecular junctions. *Science* **301,** 1221–1223 (2003).
6. Haiss, W. *et al.* Measurement of single molecule conductivity using the spontaneous formation of molecular wires. *Phys. Chem. Chem. Phys.* **6,** 4330–4337 (2004).
7. Haiss, W. *et al.* Precision control of single-molecule electrical junctions. *Nature Mater.* **5,** 995–1002 (2006).
8. Sini, G., Maitre, P., Hiberty, P. C. & Shaik, S. S. Covalent, ionic and resonating single bonds. *J. Mol. Struct. Theochem* **229,** 163–188 (1991).
9. Shaik, S., Danovich, D., Wu, W. & Hiberty, P. C. Charge-shift bonding and its manifestations in chemistry. *Nature Chem.* **1,** 443–449 (2009).
10. Shurki, A., Hiberty, P. C. & Shaik, S. Charge-shift bonding in group IVB halides: a valence bond study of MH_3–Cl (M = C, Si, Ge, Sn, Pb) molecules. *J. Am. Chem. Soc.* **121,** 822–834 (1999).
11. Fischer, H. & Radom, L. Factors controlling the addition of carbon-centered radicals to alkenes—an experimental and theoretical perspective. *Angew. Chem. Int. Edn* **40,** 1340–1371 (2001).
12. Lai, W., Li, C., Chen, H. & Shaik, S. Hydrogen-abstraction reactivity patterns from A to Y: the valence bond way. *Angew. Chem. Int. Edn* **51,** 5556–5578 (2012).
13. Warshel, A. *et al.* Electrostatic basis for enzyme catalysis. *Chem. Rev.* **106,** 3210–3235 (2006).
14. Hirao, H., Chen, H., Carvajal, M. A., Wang, Y. & Shaik, S. Effect of external electric fields on the C–H bond activation reactivity of nonheme iron–oxo reagents. *J. Am. Chem. Soc.* **130,** 3319–3327 (2008).
15. Lai, W., Chen, H., Cho, K.-B. & Shaik, S. External electric field can control the catalytic cycle of cytochrome P450cam: a QM/MM Study. *J. Phys. Chem. Lett.* **1,** 2082–2087 (2010).
16. Fried, S. D., Bagchi, S. & Boxer, S. G. Extreme electric fields power catalysis in the active site of ketosteroid isomerase. *Science* **346,** 1510–1514 (2014).
17. Klinska, M., Smith, L. M., Gryn'ova, G., Banwell, M. G. & Coote, M. L. Experimental demonstration of pH-dependent electrostatic catalysis of radical reactions. *Chem. Sci.* **6,** 5623–5627 (2015).
18. Franchi, P., Mezzina, E. & Lucarini, M. SOMO–HOMO conversion in distonic radical anions: an experimental test in solution by EPR radical equilibration technique. *J. Am. Chem. Soc.* **136,** 1250–1252 (2014).
19. Alemani, M. *et al.* Electric field-induced isomerization of azobenzene by STM. *J. Am. Chem. Soc.* **128,** 14446–14447 (2006).
20. Gorin, C. F., Beh, E. S. & Kanan, M. W. An electric field-induced change in the selectivity of a metal oxide-catalyzed epoxide rearrangement. *J. Am. Chem. Soc.* **134,** 186–189 (2012).
21. Nicolaou, K. C., Snyder, S. A., Montagnon, T. & Vassilikogiannakis, G. The Diels–Alder reaction in total synthesis. *Angew. Chem. Int. Edn* **41,** 1668–1698 (2002).
22. Paddon-Row, M. N. Investigating long-range electron-transfer processes with rigid, covalently linked donor-(norbornylogous bridge)-acceptor systems. *Acc. Chem. Res.* **27,** 18–25 (1994).
23. Darwish, N., Paddon-Row, M. N. & Gooding, J. J. Surface-bound norbornylogous bridges as molecular rulers for investigating interfacial electrochemistry and as single molecule switches. *Acc. Chem. Res.* **47,** 385–395 (2014).
24. Darwish, N. *et al.* Observation of electrochemically controlled quantum interference in a single anthraquinone-based norbornylogous bridge molecule. *Angew. Chem. Int. Edn* **51,** 3203–3206 (2012).
25. Darwish, N. *et al.* Probing the effect of the solution environment around redox-active moieties using rigid anthraquinone terminated molecular rulers. *J. Am. Chem. Soc.* **134,** 18401–18409 (2012).
26. Darwish, N. *et al.* Electroactive self-assembled monolayers of unique geometric structures by using rigid norbornylogous bridges. *Chemistry* **18,** 283–292 (2012).
27. Díez-Pérez, I. *et al.* Rectification and stability of a single molecular diode with controlled orientation. *Nature Chem.* **1,** 635–641 (2009).
28. Donhauser, Z. J. *et al.* Conductance switching in single molecules through conformational changes. *Science* **292,** 2303–2307 (2001).
29. Claridge, S. A., Schwartz, J. J. & Weiss, P. S. Electrons, photons, and force: quantitative single-molecule measurements from physics to biology. *ACS Nano* **5,** 693–729 (2011).
30. Tao, N. J. Electron transport in molecular junctions. *Nature Nanotechnol.* **1,** 173–181 (2006).

Supplementary Information is available in the online version of the paper.

Acknowledgements This research was supported by the MINECO Spanish National Project (no. CTQ2012-36090) and an EU Reintegration Grant (FP7-PEOPLE-2010-RG-277182), and by resources provided at the NCI National Facility systems at the Australian National University through the National Computational Merit Allocation Scheme, supported by the Australian Government. N.D. thanks the European Union for a Marie Curie IIF Fellowship. I.D.-P. thanks the Ramon y Cajal program (MINECO, no. RYC-2011-07951) for financial support. S.C. thanks the University of Wollongong for a Vice Chancellor Fellowship, and the Australian National Fabrication Facility for financial support. A.C.A. thanks the Spanish Ministerio de Educación for an FPU fellowship. M.L.C acknowledges financial support from the Australian Research Council (ARC) and an ARC Future Fellowship, and discussions with M. Banwell. We also acknowledge funding from the ARC Centre of Excellence Scheme (project no. CE 140100012).

Author Contributions A.C.A., N.D. and I.D.-P. carried out the STM experiments and analysed the data. N.J.B. and N.L.H. performed the quantum-chemical modelling, with input from M.L.C. S.C. carried out the synthetic work. All authors conceived the work, and designed and discussed the experiments. M.L.C. and S.C. wrote the manuscript, with substantial contributions from the other authors.

Author Information Reprints and permissions information is available at www.nature.com/reprints. The authors declare no competing financial interests. Readers are welcome to comment on the online version of the paper. Correspondence and requests for materials should be addressed to M.L.C. (michelle.coote@anu.edu.au), I.D.-P. (isma_diez@ub.edu), N.D. (ndarwish@ibecbarcelona.eu) or S.C. (sciampi@uow.edu.au).

doi:10.1038/nature16989

2. STM single-molecule junctions - additional data and control experiments

2.1. Blinking measurements at different biases.

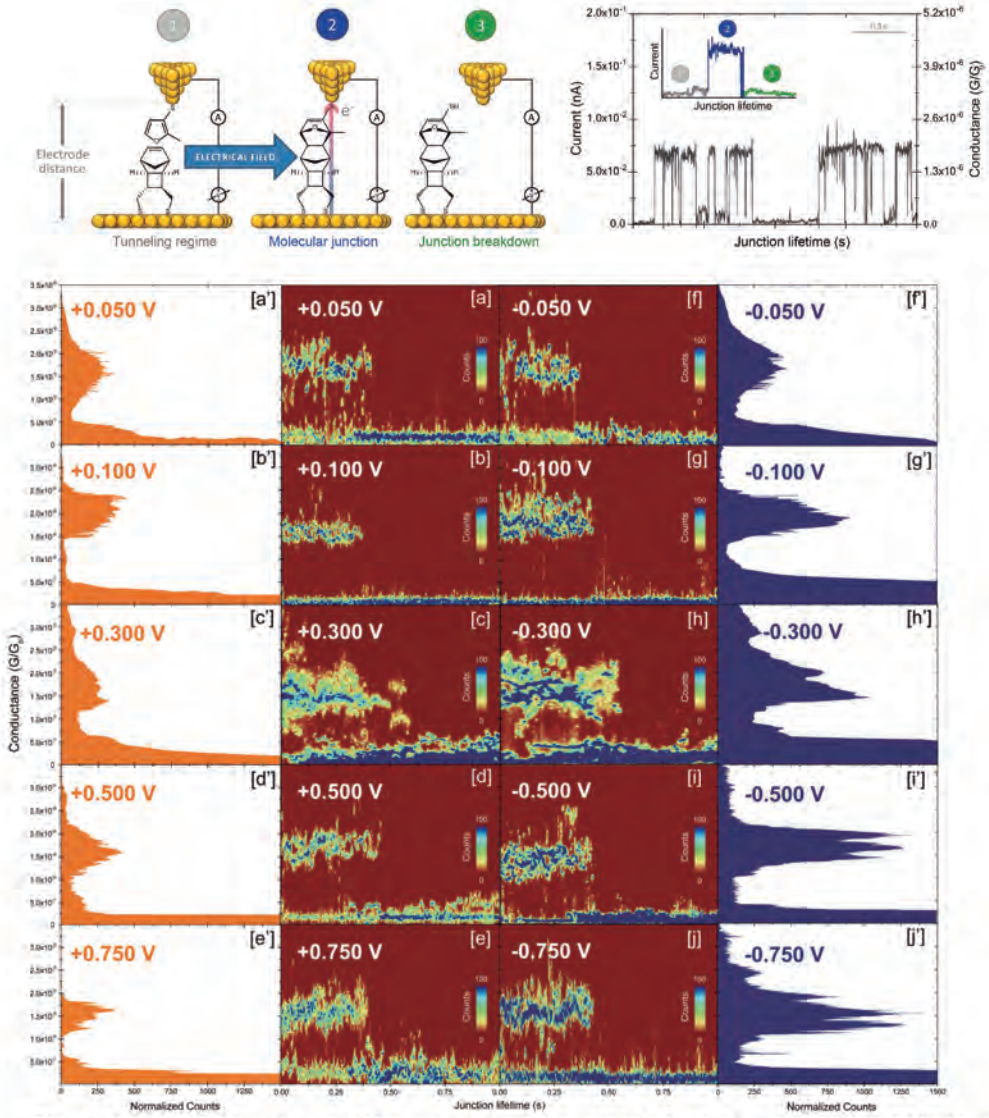

Figure S2-1. Blinking data at different biases. 2D maps obtained from hundreds of blinking events at different biases (**a-j**). Biases are indicated in the figures. Counts (color legend) have been normalized versus the total amount using 100 % as the maximum normalized value. Data were accumulated during an experimental time of 8 h for each bias. To keep the distance between the surface and the tip constant in all the bias ranges, the same set point

doi:10.1038/nature16989

current at the same initial bias was used and then the bias was changed to the specific values under feedback off. (**a'-j'**) show the corresponding 1D linear histograms obtained from the same data used to accumulate the 2D maps.

doi:10.1038/nature16989

2.2. Control tapping measurements in the absence of either reactant from the tip or from the surface

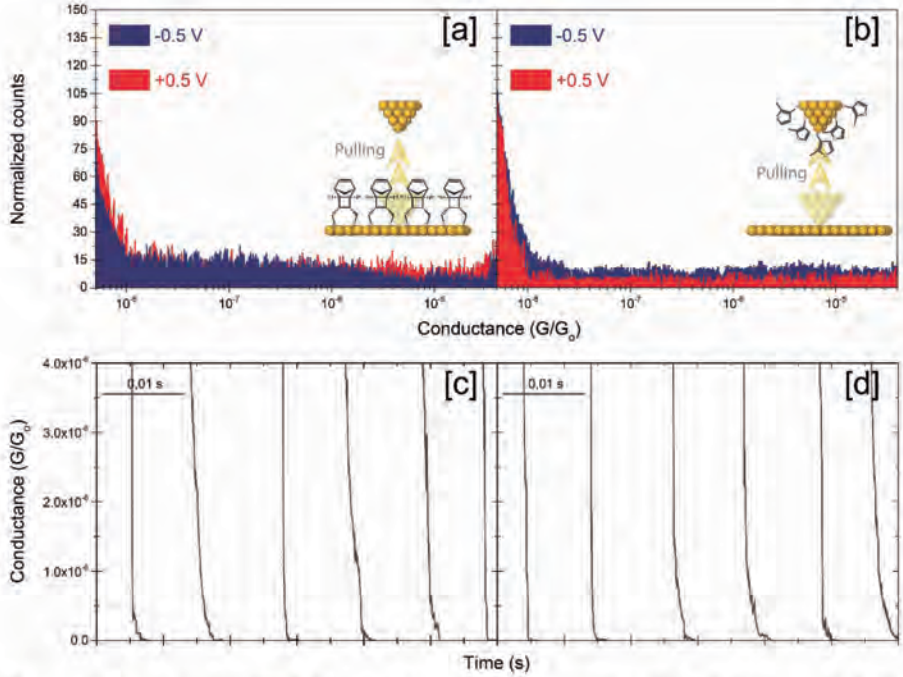

Figure S2-2. Dynamic STM-BJ control experiments. (**a**) Semilog 1D histograms built from 6000 of pulling captures that were accumulated either in the absence of the furan (diene) molecule or (**b**) in the absence of the **NB** (dienophile) molecule. (**c,d**) Representative pulling curves used to create the histograms in panels (a) and (b), respectively. Conductance plateaus are absent from the pulling curves, hence there is no evidence of formation of adducts (i.e. molecular junctions) in both type of controls. The controls indicate the need of both reactants to be simultaneously present for a junction event to occur. The surface bias is shown in the figure legends.

doi:10.1038/nature16989

2.3. Control blinking measurements in the absence of either reactant from the tip or from the surface

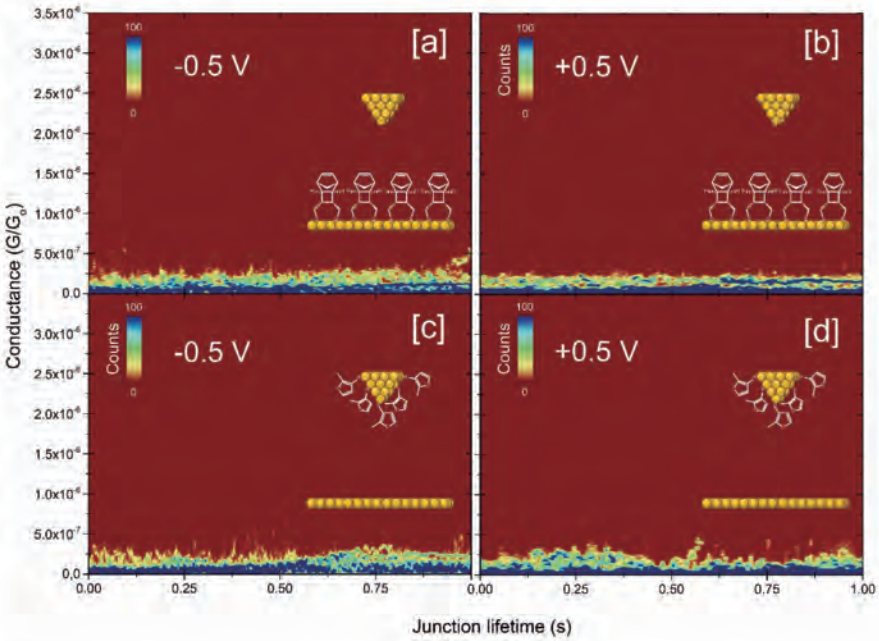

Figure S2-3. Control static "blinks" experiments. (**a**,**b**) 2D maps of blinking experiments performed either in the absence of the furan molecule on the STM tip or (**c**,**d**) in the absence of the **NB** molecule on the surface. Accumulation time was 8 h. No evidence of "blinks" was found when either of the reactants is deliberately omitted. The lack of a measurable blinking rate in the controls does strongly reinforce the assignment of the "blinks" (Fig. 3, main text, and Figure S2-1, SI) to the putative Diels-Alder event under a static field.

doi:10.1038/nature16989

2.4. Control tapping measurements with either a saturated "furan" replacing the aromatic furan or with a saturated norbornylogous bridge replacing the NB dienophile

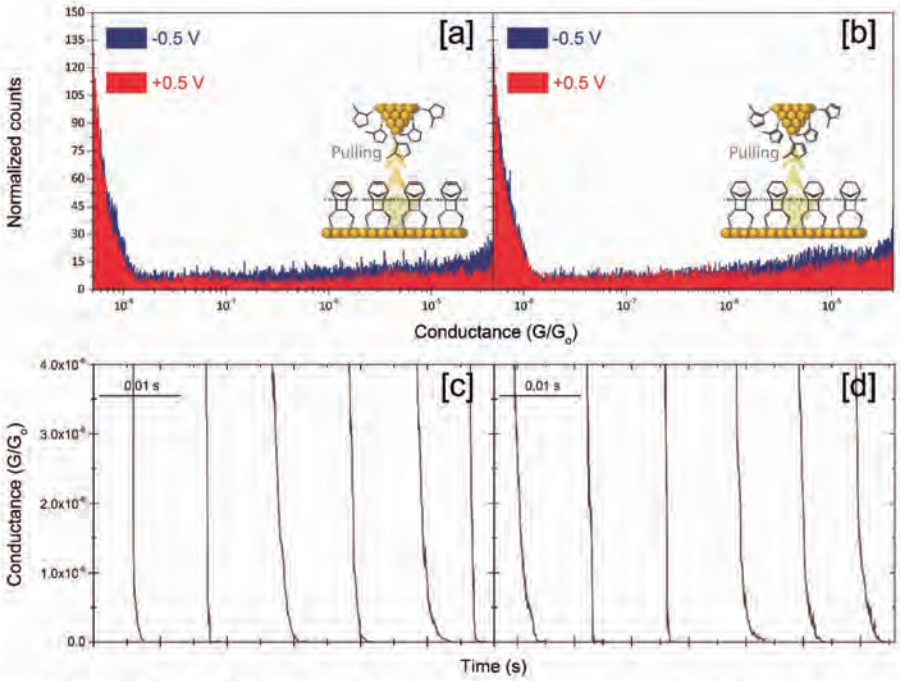

Figure S2-4. Dynamic STM-BJ control experiments. (**a**) Semilog 1D histograms built from 6000 of pulling captures that were accumulated in the presence of a "furan" molecule deprived from its diene character (2-methyl-3-tetrahydrofuranthiol) on the STM tip instead of the Diels-Alder reactive furan (diene, 2-methyl-3-furanthiol) or (**b**) in the presence of the saturated ***hydro*-NB** derivative (distal double bond in **NB** is deliberately hydrogenated) on the surface. (**c,d**) Respresentative pulling curves showing no formation of adducts (*i.e.*, molecular junctions) in both type of controls, hence indicating that single-molecule reactions only occur when both the diene and the dienophile are present.

doi:10.1038/nature16989

2.5. Blinking measurements when either a saturated "furan" is replacing the aromatic furan or when a saturated nornornylogous bridge is replacing the NB dienophile

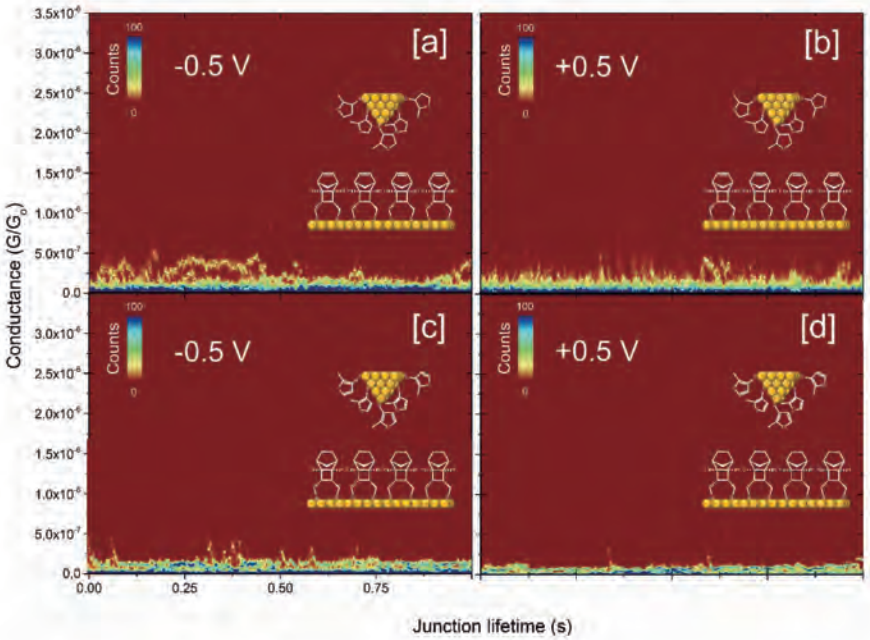

Figure S2-5. Control static "blinks" experiments. (**a-d**) 2D maps of blinking experiments performed on a system in which the aromatic furan (diene, 2-methyl-3-furanthiol, **a,b**) is replaced by its saturated, hence Diels-Alder unreactive, analogue (2-methyl-3-tetrahydrofuranthiol) or when the **NB** molecule is replaced by its hydrogenated derivative (**NB** with the double bond deliberately hydrogenated, ***hydro*-NB, c,d**). Accumulation time was 8 h, bias magnitude and direction is specified in figure. There was no evidence of formation of adducts (*i.e.* molecular junctions) in both type of controls, again indicating that the blinking events, as shown in both Fig. 3 and Figure S2-1, are only observed when both the diene and dienophile are simultaneously present. This rules out the possibility of side-reactions giving signals in the 1.5×10^{-6} G_o conductance range.

doi:10.1038/nature16989

2.6. Pulling curves during a blinking event and during a STM-BJ dynamic approach measurement.

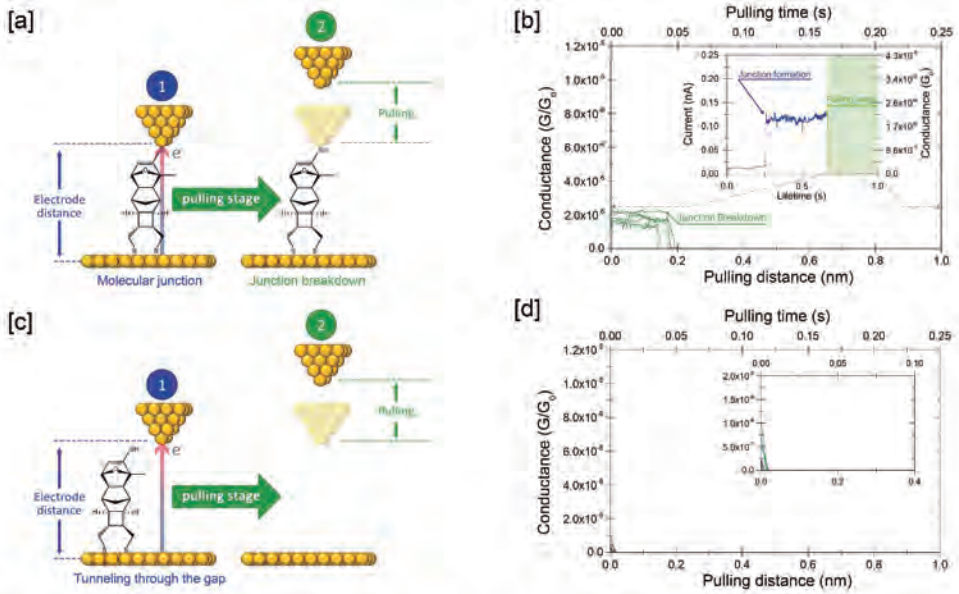

Figure S2-6. Mechanical pulling over blinking and non-blinking events. (**a**) Schematic of the pulling stage over a blinking event: (1) during the formation of a junction when the product is formed and before the pulling stage; (2) junction breakdown when the tip is pulled away from the surface. (**b**) Representative pulling curves during the blinking events at 1.5×10^{-6} G_0. The inset shows the blink before and after the pulling stage. As shown in Figure S2-b, the blink can be stretched by ~ 0.2 nm which demonstrate that the junction possess significant mechanical resistance to the pulling attempt and testify for the formation of robust molecular junction between the 2 electrodes. This behavior is in contrast to (**c**) pulling performed when the current is showing only the tunneling current background without a product molecule connected between the electrodes which results immediately in an (**d**) an exponential decay in the current without any mechanical resistance.

doi:10.1038/nature16989

2.7. STM-BJ dynamic approach measurement.

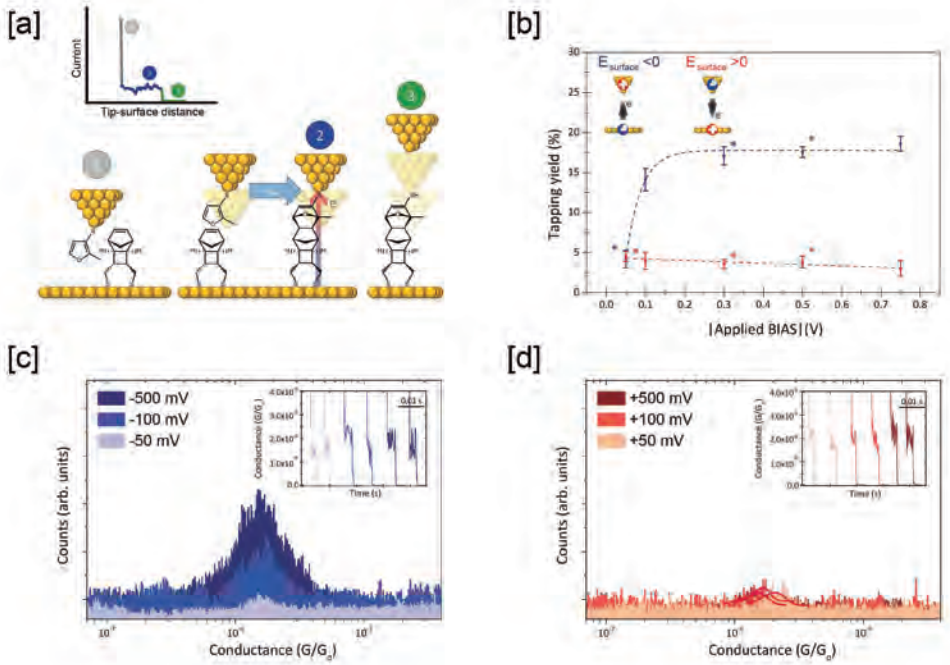

Figure S2-7. Tapping experiments under different electrical fields. (a) Schematic of the STM-BJ dynamic "pulling curves" approach: (1) tip and surface in contact, (2) during the formation of a junction when the two reactants are joined and (3) junction breakdown when the tip is pulled away from the surface. The inset represents the corresponding current response during the three stages: (1) current saturation, (2) current plateau and (3) zero current stage. **(b)** Tapping yield (number of molecular junctions formed / total number attempts) at different negative and positive biases. 6000 attempts were performed for each bias. **(c,d)** Semilog 1D histograms obtained from the pulling captures (c) for negative surface bias and (d) for positive surface bias. Insets in (c) and (d) show representative pulling captures in linear scale. The asterisks in figure (b) indicate the selected biases depicted in figures (c) and (d).

5.3 Findings and Discussion

— *The main findings of this study were the following:*

- The only detected current signal was determined at 1.5-2x10^{-6}G$_0$ and all the single-current measurements were based on this current signature.

- From the *blinking* approach experiments, under the *tip-to-substrate* EEF orientation in the defined range from the -0.050 V to -0.750 V of bias (15-fold voltage range), the observed number of *blinking* events per time increased until reach a 5-fold asymptotic maximum. Furthermore, under the *substrate-to-tip* EEF orientation the number of *blinking* events per time kept a constant value over the range of -0.050 V to -0.750 V of bias (15-fold voltage range).

- Employing the *tapping* approach the showed behaviors under both EEF orientation were similar to the obtained by *blinking* approach. The observed behavior for the *substrate-to-tip* EEF orientation of ca. 4% product formation (total events/junction events) increased asymptotically to ca. 19% under *from-tip-to substrate* EEF orientation, representing an increment of the reaction rate of ca. 4.4-fold.

- The computational results show eight potential Diels-Alder product isomers, four enantiomeric forms for each *exo/syn*, *exo/anti*, *endo/syn* and *endo/anti* with two diastereoisomers each one according to the localization of the furan substituent on the left or on the right side of the molecule. From the calculated energy values, only the two *exo/syn* products of this reaction are kinetically favored products, the other six possible products present much higher reaction barriers over the experimental range of field strengths. Two possible resonance structures of the transition state for the *exo/syn* diastereoisomers present dependence on their stabilization energy according the EEF polarization, this is because each structure's charge distribution is sensitive to different EEF orientation, nevertheless the stabilized under negative biased EEF presents a lower reaction barrier.

— *The discussion of the results is summarized below:*

- From the calculations can be assumed that the two possible *exo/syn* diastereoisomers structures are not affected equally by the EEF. The *right-handed furan substituted* structure shows strong field sensitivity, while the formation of the *left-handed furan substituted* structure is quite insensitive to the experimental range of field strengths, both cases as a consequence of the favorable or unfavorable orientation of the bond vector respect the EEF lines, respectively. The orientation effects of the EEF over *right-handed furan substituted* structure depend on the two minor resonance contributors stabilization. Inside the applied experimental bias range of few V·nm^{-1}, the energy barrier for one

the possible contributors is lowered only under negative bias voltages (*from tip-to-substrate* oriented EEF) in which the dienophile bears a positive charge and the diene carries a negative charge. The other possible contributor due its less inherent stability only can be stabilized under positive bias voltages (*from substrate-to-tip* oriented EEF), but out of the experimental bias voltage margins. In summary, inside the experimental range only can be stabilized one contributor and it happens specifically under negative bias voltages.

- The employed *set-up* under the applied conditions allowed to carry out the Diels-Alder reactions from individual reactant molecules attached to the electrodes. With supporting procedures and several control experiments was determined that the only certainly detected reaction was the Diels-Alder, followed via current measurements using the current signature of 1.5-2x$10^{-6}G_0$ associated to the product molecule trapped between the electrodes, junction assessed through the different performed control experiments.

- The net effect of the two diastereoisomers is the increment of the detected reaction rate according to the bias voltage magnitude and only under negative voltages (*from tip-to-substrate* oriented EEF), as was assessed through the increase of the *"blinking events"* or *"tapping yield"*. Distinguish experimentally between both diastereoisomers was not possible with the used current detection method, so can be assumed that the detected current signal comprises the contribution of both structures. The *light-handed furan substituted* diastereoisomer not affected by EEF can be associated to a minimal and constant detection of current signal events, analogous to its continuous formation; contrary, the *right-handed furan substituted* diastereoisomer presents a variable current signal events associated to its dependence to the EEF, which increases only under negative bias voltages (*from tip-to-substrate* EEF) causing the increasing to the detected total number of events.

- Despite the qualitative obtained results, the observed trend in the frequency of the detected events are enough sginificant to establish a direct relation with the reaction rate trend. This is because the exact number of molecular reaction events are not possible to quantify since exist some limitations inherent to STM-BJ technique which can affect to the qualitative analysis. Regarding the lowest reaction rates, the employment of saturated functionalized electrodes can induce the reaction thus biasing the results, specially using *tapping* due the mechanically forced reaction. Regarding the highest reaction rates, the technique by itself presents a limitation due the capturing frequency of the used amplifiers because they only capture events slower than its maximum time resolution, as a consequence any current event occurred in a higher frequency than the threshold will not be captured. In addition, *tapping* approach's maximum achieved yield to form a molecular junction is around the 20% of the total attempts.[50,111,361,564,565] Nevertheless, since the obtained trend employing both approaches is equivalent and both can affect the captures in different ways, is assumed that the obtained results are not significantly biased.

5.4 Conclusions of the Chapter

The presented work in this Chapter represents the first experimental evidence of how a controllable EEF as external stimulus affects to the Diels-Alder reaction barrier at RT, elucidating the capacity of the EEF to electrostatically stabilize a minor charge-separated resonance contributor of the transition state of a non-redox reaction, as Shaik's theory predicts. This, opens the gate to an efficient application of the electrostatic catalysis field and the possibility to study the effects of the EEF on other bimolecular reactions at the *nanoscale* as well as the future prospects to apply the EEF effects on a bulky dimension. Is important highlight that the novelty of the presented work is not only the experimental attest of the EEF effects, also the presented methodology and the adapted STM-BJ *set-up* have a remarkable contribution because it allows the appropriately settlement of the reactant molecules as well as the control of the EEF in strength and orientation; emphasizing the significant role the sharpness of the tip and the attained meticulous nanometric separation between the tip and the substrate electrodes, because both favor the electron flow from the dienophile to the diene with a strong and directional electric field for the implied molecules This proposed new platform to study and control chemical bimolecular reactions at the single-molecule level, might can help to provide in the future unprecedented information about reaction mechanisms to the scientific community. The next immediate step is the adaptation of the developed single-molecular detection platform and the learned new concepts about how to orient and manipulate the EEF, to the enzymatic catalysis since their evident similitudes. Enzymatic catalysis is based on oriented LEF created by strategically located charged residues, which interact specifically with a reactant (*substrate*) and stabilizes the TS, thus the observed EEF phenomenology can serve as the first step to expand the nanocatalysis field to the biological enzymatic models, being a long term aim of the performed study due its economical implications.

Focusing on the findings, this conclusive research is a proof-of-concept of an old theoretical prediction achieved experimentally where the experimental results and the observed trend are qualitatively consistent with theoretical calculation predictions. Now is possible affirm that EEF both strength and orientation can affect to chemical reactions, and the implicit conclusions of the research are listed as follows:

- Diels-Alder reaction can be accelerated via controlling two variables at the same time: the EEF orientation *(i)* aligned in the specific way respect to the reaction center and pointing from the *diene* (bearing a negative charge) to the *dienophile* (bearing a positive charge) and the field strength *(ii)* to tune the reaction processes.

- Some potential parameters which can affect to the reaction rates are not studied in this investigation and should be further studied. Qualitatively, these candidates could be: the alterations on the produced electric field between the tip and substrate electrodes due their dissimilar shape, the attachment of the reactant molecules to inverted electrode dispositions modifying the bond

vector direction respect the EEF orientation, the effects over the contributors stabilization due the organic medium and also the effects of both current magnitude and generated heat, associated to the applied bias voltage magnitude.

- Since the EEF control can be used specifically to manipulate chemical reactions and tune *in-situ* the reaction rates at single-molecule level, represents the proof-of-principle to convert a current detection instrument such the STM onto a real single-molecule nano-reactor device, conveniently capable to tune both chemical reactivity and selectivity supported by computing and/or theory predictions, and even could be considered a sort of a very initial stage of a future molecular assembling machine.

- The obtained results are a consequence of a large and directional created electric field proportional to the molecular scale and the STM's electrodes *nanogap*, therefore the applied field strength should be increased proportionally to larger scales to be suitable for *Industrial-Scale* Synthesis.